NANO LETTERS

Letter

pubs.acs.org/NanoLett

Hybrid Photon-Plasmon Nanowire Lasers

Xiaoqin Wu,[†,§] Yao Xiao,[†,§] Chao Meng,[†] Xining Zhang,[†] Shaoliang Yu,[†] Yipei Wang,[†] Chuanxi Yang,[†] Xin Guo,[†] C. Z. Ning,[‡] and Limin Tong*[,†]

[†]State Key Laboratory of Modern Optical Instrumentation, Department of Optical Engineering, Zhejiang University, Hangzhou 310027, China

[‡]School of Electrical, Computer, and Energy Engineering, Arizona State University, Tempe, Arizona 85287, United States

Supporting Information

ABSTRACT: Metallic and plasmonic nanolasers have attracted growing interest recently. Plasmonic lasers demonstrated so far operate in hybrid photon-plasmon modes in transverse dimensions, rendering it impossible to separate photonic from plasmonic components. Thus only the far-field photonic component can be measured and utilized directly. But spatially separated plasmon modes are highly desired for applications including high-efficiency coupling of single-photon emitters and ultrasensitivity optical sensing. Here, we report a nanowire (NW) laser that offers subdiffraction-limited beam size and spatially separated plasmon cavity modes. By near-field coupling a high-gain CdSe NW and a 100 nm diameter Ag NW, we demonstrate a hybrid photon-plasmon laser operating at 723 nm wavelength at room temperature, with a plasmon mode area of $0.008\lambda^2$. This device simultaneously provides spatially separated photonic far-field output and highly localized coherent plasmon modes, which may open up new avenues in the fields of integrated nanophotonic circuits, biosensing, and quantum information processing.

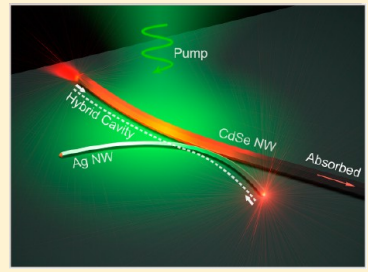

KEYWORDS: *Plasmon, laser, nanowire, hybrid cavity, subdiffraction limit*

As coherent sources that can provide optical-frequency radiation well below the classical diffraction limit in one or more spatial dimensions, nanoscale plasmonic lasers have been attracting more and more attentions in the past few years.[1−15] Relying on diverse configurations of metallic nanostructures (such as clads,[5,10] films,[7,9,11−13] stripes,[8] and particles[6,15]) adjacent to certain gain media, deep-subdiffraction nanolasers have been successfully demonstrated. However, all the plasmonic lasers reported so far operate in hybrid photon-plasmon modes in the direction transverse to the propagation direction, making it impossible to separate a pure plasmon cavity mode from photonic component. Consequently, only the far-field photonic component can be measured and utilized directly.

For practical applications, direct access to a plasmon cavity mode is an important approach to provide nanoscale confined fields for light-matter interactions. Moreover, within visible and near-infrared spectral range the relaxation time of the plasmon oscillation in metals can go down to ∼10 fs level,[16,17] which offers an opportunity for modulating a laser containing separated plasmon cavity modes with ultrahigh rates. Therefore, nanolasers with spatially separated plasmon cavity modes are highly potential for wide applications including strong coupling of quantum nanoemitters,[18−23] ultrasensitivity optical sensing,[24−27] and ultrafast-modulated coherent sources.[17,28,29]

Chemically synthesized nanowires (NWs) offer excellent surface smoothness and crystalline structures, which ensure low waveguiding losses for both photonic[30] and plasmonic[31,32] modes. For plasmonic waveguiding, Ag NWs are of particular interest owing to their low dissipative loss (Ohmic loss) in the visible and near-infrared ranges.[33] Also, the polaritonic resonances[16] of Ag NWs match the gain spectral range of some high-gain ($>10^3$ cm^{-1}) semiconductor[7,11−13] (e.g., CdSe) NWs, making it possible to compensate the Ohmic loss of the metal for lasing actions in a hybrid photon-plasmon NW cavity.

By near-field coupling a long CdSe NW and a 100 nm-diameter Ag NW, here we demonstrate a hybrid photon-plasmon NW laser that offers subdiffraction-limited beam size and spatially separated plasmon modes. The laser operates around 723 nm wavelength at room temperature and offers far-field-accessible pure plasmon cavity modes on a 3.7 μm length Ag NW with a beam size of $0.008\lambda^2$. We also show that the hybrid photon-plasmon NW laser can be modulated by solely modifying the propagation loss of the plasmon modes in the Ag NW.

Here, the hybrid photon-plasmon NW laser we proposed is schematically illustrated in Figure 1. A Ag NW is side-coupled to an ultralong CdSe NW to form an X-shape structure (Figure 1a). The coupling point is located close to the left end of the CdSe NW, dividing the NW into two segments: the shorter one to the left serves as a gain medium under optical pump; the longer one to the right that is outside the pump beam and highly absorptive around the emission band of the CdSe[34,35] serves as a distributed absorber to eliminate reflection from the right side of the NW.[36] As shown in Figure 1b, the photoluminescence (PL) from CdSe band-edge is waveguided

Received: September 5, 2013
Revised: October 11, 2013
Published: October 17, 2013

   dx.doi.org/10.1021/nl403325j | *Nano Lett.* 2013, 13, 5654−5659

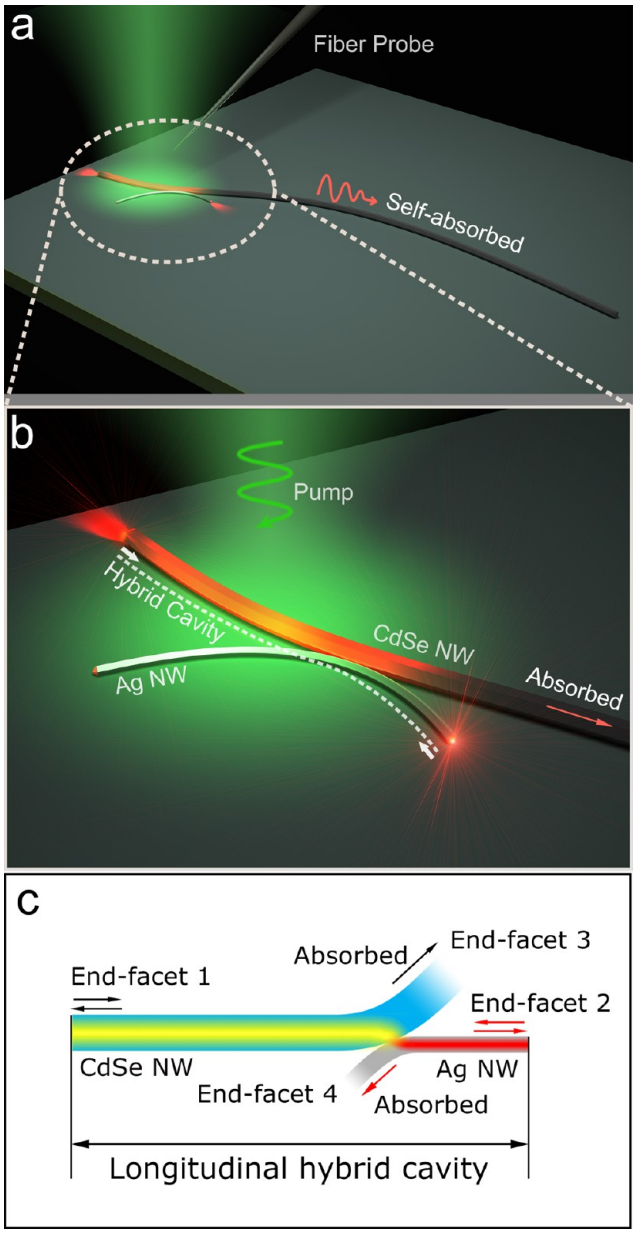

Figure 1. Schematic illustration of a hybrid photon-plasmon NW laser. (a) The hybrid photon-plasmon NW laser is composed of a Ag NW and an ultralong CdSe NW coupled into X-shape using a fiber probe for micromanipulation. The right segment of CdSe NW serves as a distributed absorber without reflection. (b) Closed-up view of the coupling area indicating the coupled hybrid cavity (marked by the dashed line), which serves as the hybrid photon-plasmon lasing cavity. (c) Cavity formation in the X-structure.

along the NW until reaching the joint area, where the photon modes of the CdSe NW are coupled and converted into plasmon modes of the Ag NW.[37] The reflection of plasmon modes at the right end of the Ag NW[22,31,38] and photon modes at the left end of the CdSe NW[39] alternately recirculates photon and plasmon modes for lasing oscillation in this longitudinal hybrid cavity. A key difference between plasmonic nanolasers reported before[5−14] and the one shown here lies in the way plasmonic and photonic components are coupled. In the former, photonic and plasmonic components are hybridized in the transverse direction and spatially inseparable, here the photon cavity mode (within CdSe NW) and plasmon cavity mode (within Ag NW) are hybridized along the longitudinal direction and thus spatially separated. Above the threshold, the bidirectional propagation constantly converts energy between the photonic and plasmonic components, providing spatially separated photonic far-field output from the end of CdSe NW, while highly localized coherent plasmon modes from the end of Ag NW simultaneously.

Generally, when the CdSe NW is excited, a large fraction of PL is channeled into guided modes and reflected at the end-facets of both CdSe and Ag NWs, which may form four resonant cavities (end-facet 1 to end-facet 2, end-facet 1 to end-facet 3, end-facet 4 to end-facet 2, end-facet 4 to end-facet 3, as shown in Figure 1c) in the X-structure.[36] Here, the pumping light is focused on the left segment of the CdSe NW, while the right segment (outside the focusing area) is served as a nonreflective absorber. Thus, only one active cavity that consists of the left segment of the CdSe NW and the right segment of the Ag NW (i.e., end-facet 1 to end-facet 2) works.

Experimentally, chemically synthesized CdSe NW[40] is cut with a flat end facet using a bend-to-fracture process[41] (Figure 2a), and emission from individual NW end-facets is measured by a selected-area spectral measurement system (Supporting Information Figure S1). The PL of the CdSe NW is centered around 722 nm with a full width at half-maximum (fwhm) of 18 nm (Figure 2b). The Ag NW is prepared by a solution-phase method[42] with excellent diameter uniformity and sidewall

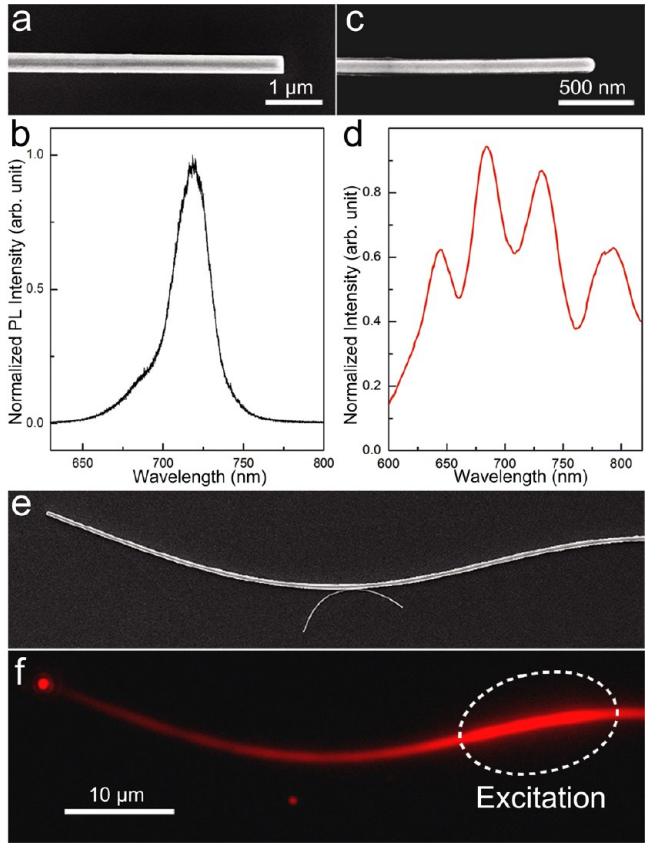

Figure 2. (a) Scanning electron microscopy (SEM) image of one end of a 390 nm diameter CdSe NW. (b) PL spectrum of the CdSe NW in (a). (c) SEM image of one end of a 100-nm-diameter Ag NW. (d) F–P resonance spectrum of the Ag NW in (c). (e) SEM image of a coupled hybrid cavity composed of a CdSe and Ag NW. (f) Optical characterization of the coupled structure.

dx.doi.org/10.1021/nl403325j | *Nano Lett.* 2013, 13, 5654−5659

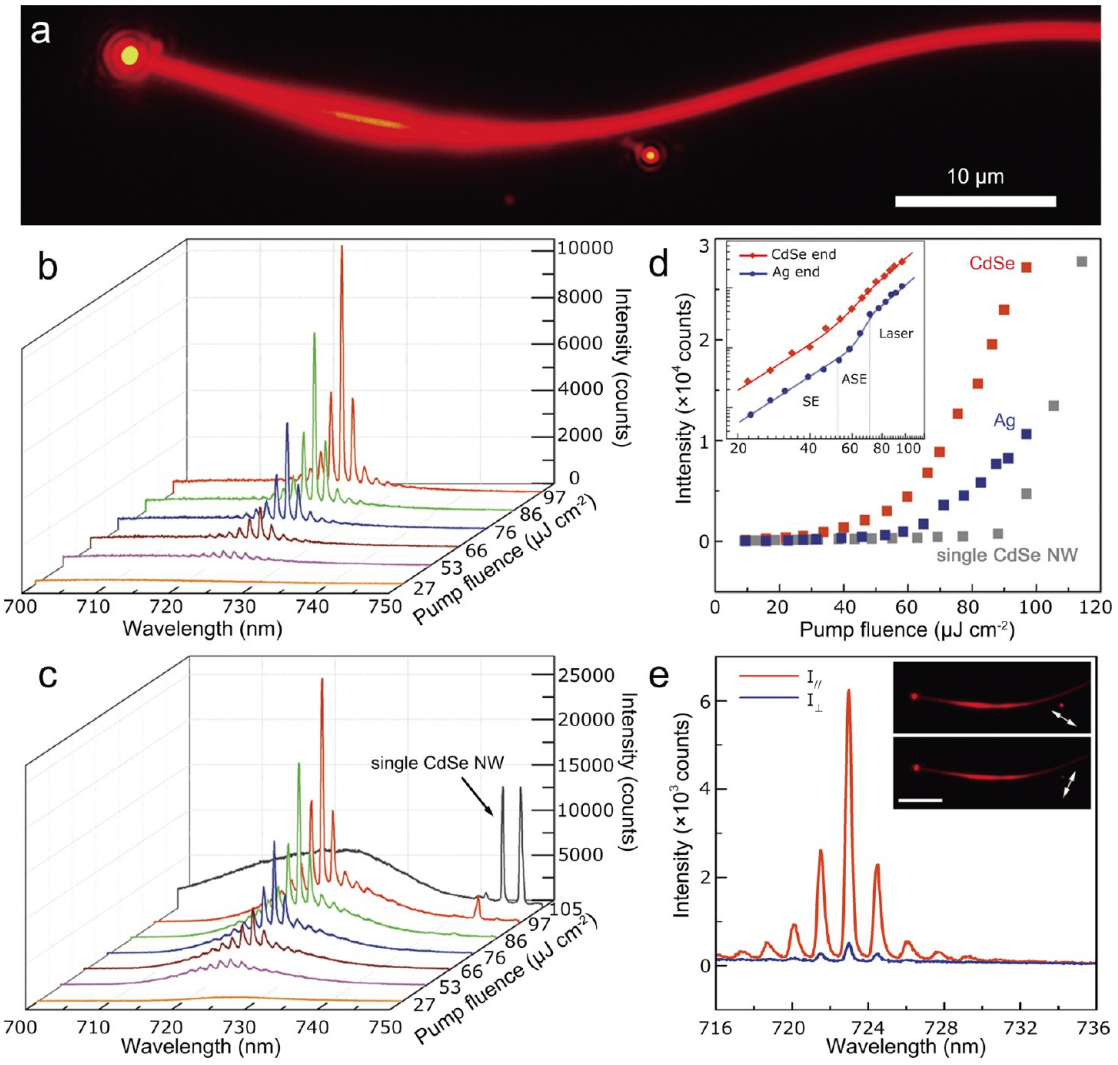

Figure 3. Lasing characterization of the hybrid photon-plasmon nanowire laser. (a) Optical microscope image of the lasing structure under a pump fluence of 97 μJ cm^{-2} (19.4 KW cm^{-2}) with an exposure time of 15 s. (b) Lasing spectra collected from the Ag end-facet under pump fluences of 27−97 μJ cm^{-2}. (c) Lasing spectra collected from the CdSe end-facet under pump fluences of 27−97 μJ cm^{-2} (orange to red line). The gray line spectrum is from the individual CdSe NW before coupling to the Ag NW under pump fluence of 105 μJ cm^{-2}. (d) Emission intensity versus pump fluence collected from end-facets of the CdSe NW (red squares) and the Ag NW (blue squares), according to the dominant lasing peak centered around 723 nm. The gray-square pattern is from the individual CdSe NW before coupling to the Ag NW, according to the dominant lasing peak centered around 745 nm. The inset shows the same data from CdSe and Ag ends on a log−log scale. (e) Polarization-sensitive lasing spectra from Ag NW end-facet with the emission polarization oriented parallel (red line) and perpendicular (blue line) to the Ag NW. Inset, dark-field microscope images show the polarization-dependent lasing outputs. The exposure time is 1 s and the scale bar is 10 μm. The white arrows indicate the directions of the polarization.

smoothness (Figure 2c). From Fabry−Perot (F−P) resonance spectrum (Figure 2d), we estimate a facet reflectivity of about 25% of a 100 nm diameter Ag NW[22,31] [see Supporting Information]. Using fiber probes for micromanipulation [see Supporting Information], the hybrid cavity is assembled from a 100 nm diameter 11 μm long Ag NW and a 390 nm diameter 470 μm long CdSe NW on a MgF_2 substrate (Figure 2e). The left segment of CdSe NW and the right segment of Ag NW are 28.6 and 3.7 μm in length, respectively. The overlap length of the two segments is about 1.1 μm, long enough for efficient photon-plasmon conversion.[37] By exciting the CdSe NW at the right side of the coupling area with a 532 nm wavelength light, we observe evident output from the Ag NW (Figure 2f) and determined a photon-to-plasmon coupling efficiency of 20% [see Supporting Information].

To investigate the lasing action, 532 nm wavelength laser pulses (5 ns pulse width, 2 kHz repetition rate) are loosely focused on the left segment of the CdSe NW (Figure 1) and the emission scattered from each end-facet is collected by the selected-area spectral measurement system (Supporting Information Figure S1). Under excitation, strong luminous spots are observed at both ends of the hybrid cavity (Figure 3a) with clear interference rings indicating strong spatial coherence of the light emitted. The output spot of the Ag NW (even with the limited spatial resolution) is much smaller than that of the CdSe NW, indicating much tighter confinement of the SPP radiation. Figure 3b,c shows typical emission spectra collected at the right end of the Ag NW and the left end of the CdSe NW, respectively. When the pumping fluence increases from 27 to 97 μJ cm^{-2}, the emission output experiences a three-stage transition[43] (Figure 3d): spontaneous emission (SE) in which

dx.doi.org/10.1021/nl403325j | Nano Lett. 2013, 13, 5654−5659

the gain from the CdSe NW is much lower than the loss of the Ag NW; amplified spontaneous emission (ASE) with cavity gain approaching the loss; and full lasing oscillation in which the output exhibits a linear dependence on the pump intensity.

The red lines in Figure 3b,c shows typical multimode lasing feature, with dominant lasing peak centered around 723 nm, and an average free space range (FSR) of 1.50 nm. Theoretically, FSR of hybrid CdSe-Ag NW cavity is given by FSR $\approx \lambda^2/2(L_{CdSe}n_{g,CdSe} + L_{Ag}n_{g,Ag})$, yielding a calculated value of 1.54 nm (see Supporting Information). The good agreement of the theoretical value and the experimental measurement (1.54 nm vs 1.50 nm) verifies that the lasing cavity is hybridized by the Ag and the CdSe NWs. The line-width of the 723 nm lasing peak is 0.38 nm, indicating the relatively high quality of the hybrid cavity. With increasing pump intensity, emission outputs from both CdSe and Ag NWs (Figure 3b,c) show a synchronous evolution from SE to lasing oscillation with almost the same lasing threshold of about 60 μJ cm^{-2} (or 12 KW cm^{-2}) (Figure 3d). It is noticed that the output from the CdSe NW has a clear PL background (Figure 3c) in contrast to that of the Ag NW (Figure 3b), which may come from the radiation mode of the PL generated in the vicinity of the end-facet. Also, under more intense pump fluence (97 μJ cm^{-2}), a small peak around 745 nm from the output of the CdSe NW (red line, Figure 3c) is observed, coinciding with the lasing peak of a single CdSe NW (gray line, Figure 3c) and indicating the coexistence of both hybrid-cavity and single-NW-cavity mode (realized by distributed feedback from the right part of the CdSe NW). For comparison, no 745 nm peak is observed in the output of the Ag NW, indicating that the output from the Ag NW is purely from the hybrid lasing cavity. More specifically, we determined that the lasing threshold of the single 470 μm long CdSe NW (before coupling to the Ag NW) is about 90 μJ cm^{-2} (gray squares, Figure 3d), much higher than 60 μJ cm^{-2} of the hybrid cavity, indicating that the feedback from the right end of the Ag NW is much higher than that from the distributed reflection from the long CdSe NW. Therefore, it is no doubt that the lasing emission with pumping intensity below 90 μJ cm^{-2} comes solely from the hybrid photon-plasmon cavity.

The polarization of the plasmon lasing output from the Ag NW is also investigated. As shown in Figure 3e, the output intensity of the Ag NW is highly polarization-dependent; compared with that along the direction perpendicular to the NW axis, the output spot of parallel polarization is much brighter (inset of Figure 3e) with a polarization ratio ($\rho = I_{//}/I_{\perp}$) as high as 92% for the 723 nm lasing mode, representing the electromagnetic feature of the pure plasmon mode.[16,20,44] In addition, with a MgF_2 substrate, the mode area of the Ag NW at the lasing wavelength λ (around 723 nm wavelength) is calculated[45] to be 0.004 μm^2 (0.008λ^2), corresponding to a mode size of 70 nm ($\sim\lambda/10$) (see Supporting Information), well below the optical diffraction limit (typically $>\lambda/5$).

To further establish the role of the Ag NW, we investigate the emission of a hybrid cavity assembled with a 284 nm diameter CdSe NW and a 140 nm diameter Ag NW by modifying the optical properties of the Ag NW. For this purpose, here we couple a second Ag NW to the right end of the first Ag NW to introduce additional loss to the first Ag NW (or equivalently increase the cavity loss) and collect emission from the left end of the CdSe NW before and after the coupling (Figure 4a,b), respectively. Measured pump-fluence-dependent output (Figure 4c) shows that without the second Ag NW, the

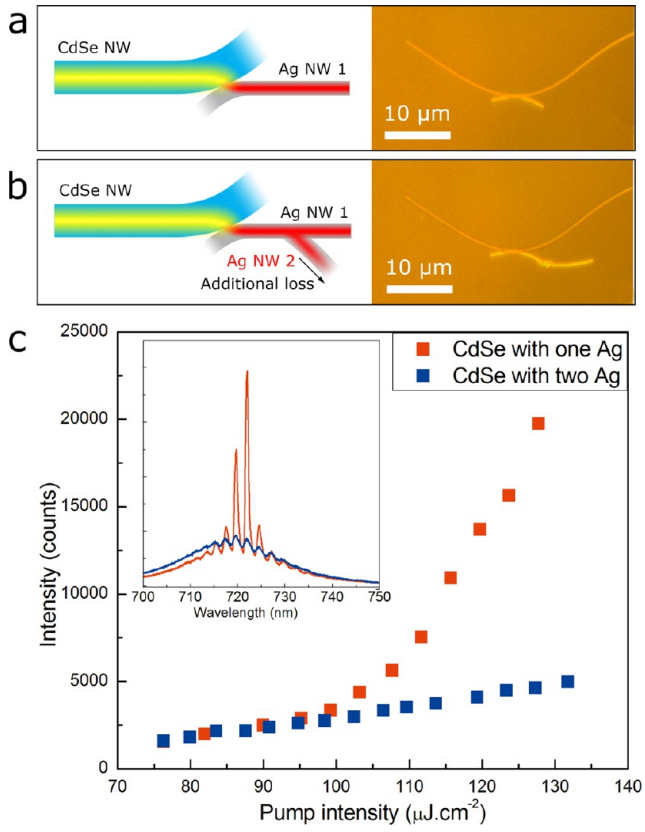

Figure 4. Schematics diagrams (left) and optical microscope images (right) of a hybrid cavity before (a) and after coupling a second Ag NW (b), respectively. (c) Output intensity collected from the left end of the CdSe NW before (red squares) and after (blue squares) coupling the second Ag NW, respectively. Inset, emission spectra collected from the left end-facet of the CdSe NW before (red line) and after (blue line) coupling a second Ag NW, under a pump fluence of 128 μJ cm^{-2}.

lasing threshold of the original hybrid cavity is about 100 μJ cm^{-2}; when the second Ag NW is coupled, the lasing oscillation disappears within the available pump fluence up to 130 μJ cm^{-2}. For comparison, inset of Figure 4 shows the typical output spectra of the two situations under the same pump fluence of 127 μJ cm^{-2}, clearly demonstrating that the Ag NW is part of the lasing cavity, rather than a passive SPP waveguide. The result also shows that the lasing oscillation can be switched off by modifying optical properties of the separated plasmon cavity mode, suggesting a possible approach to lasing modulation by directly tuning the plasmonic component.

In summary, we have established a clear case of hybrid photon-plasmon nanolaser with simultaneous and spatially separated photonic and plasmonic outputs. As part of the lasing cavity, the Ag NW can offer special merits such as ultratight confined optical fields[20,45] and ultrafast modulation in dielectric constants.[46] Our plasmonic nanolasers provide a number of unique opportunities including subdiffraction optical nonlinear effects, ultrasensitive optical sensing, and ultrafast modulation. Furthermore, the highly localized and spatially separated plasmon modes can be efficiently delivered to an application point or to other photon emitters (e.g., quantum dots) as a localized excitation source for quantum information applications.[18−22] Finally, since the spot size of a pure plasmon mode is solely determined by the diameter of the Ag NW and decreases monotonously with the NW diameter,[20,45] it is

dx.doi.org/10.1021/nl403325j | Nano Lett. 2013, 13, 5654−5659

possible to achieve a plasmonic source with a size far below the diffraction limits (e.g., molecular level[4]).

Methods. *Synthesis of CdSe and Ag NWs and Assembling of the X-Coupled Structure.* The Ag NWs used in this work were synthesized by a soft (with temperatures less than 200 °C) solution phase approach.[42] Ag NWs were deposited from solution onto an MgF_2 substrate. Then a CdSe NW synthesized by chemical vapor transport process[40] was transferred to the same substrate with a Ag NW near one end, using a pair of fiber probes for micromanipulation under a microscope equipped with a 100× objective. With the same equipment, the two NWs were assembled into X-shape structure (see Supporting Information).

Optical Measurements. To pump the plasmon laser and characterize the single CdSe NW as well, 532 nm laser pulses (2 kHz repetition rate, 5 ns pulse width) from a frequency doubled Nd:YAG laser were focused to a spot size ∼30 μm through the 100× objective (NA = 0.70), offering a pump fluence of 0−1000 $\mu J\ cm^{-2}$ in the excitation area. The PL or laser signals scattered from end-facets of CdSe and Ag NWs were collected by the same objective (see Supporting Information). All experiments were performed under room temperature.

■ ASSOCIATED CONTENT

Supporting Information

Section 1: Selected-area spectral measurement system. Section 2: End-facet reflectivity of Ag NWs. Section 3: Absorption-induced propagation loss of a CdSe NW. Section 4: Coupling efficiency between a CdSe NW and a Ag NW. Section 5: Calculation of FSR of the hybrid cavity. Section 6: Micromanipulation process of assembling the hybrid NW cavity. Section 7: Mode area estimation of the Ag NW. Figures S1−S6. This material is available free of charge via the Internet at http://pubs.acs.org.

■ AUTHOR INFORMATION

Corresponding Author

*E-mail: phytong@zju.edu.cn.

Author Contributions

§X.W. and Y.X. contributed equally to this paper.

Notes

The authors declare no competing financial interest.

■ ACKNOWLEDGMENTS

We thank Y.Y., Z.Y.Y. and Q.Y. for assistance in CdSe NW growth. This work was supported by the National Key Basic Research Program of China under Grant Agreement 2013CB328703 and the National Natural Science Foundation of China under Grant Agreements 61036012 and 61108048.

■ REFERENCES

(1) Berini, P.; De Leon, I. Surface plasmon-polariton amplifiers and lasers. *Nat. Photonics* **2012**, *6*, 16−24.

(2) Ding, K.; Ning, C. Z. Metallic subwavelength-cavity semiconductor nanolasers. *Light: Sci. Appl.* **2012**, *1*, e20.

(3) Gather, M. C. A rocky road to plasmonic lasers. *Nat. Photonics* **2012**, *6*, 708−708.

(4) Ma, R. M.; Oulton, R. F.; Sorger, V. J.; Zhang, X. Plasmon lasers: coherent light source at molecular scales. *Laser Photon. Rev.* **2013**, *7*, 1−21.

(5) Hill, M. T.; et al. Lasing in metallic-coated nanocavities. *Nat. Photonics* **2007**, *1*, 589−594.

(6) Noginov, M. A.; et al. Demonstration of a spaser-based nanolaser. *Nature* **2009**, *460*, 1110−1112.

(7) Oulton, R. F.; et al. Plasmon lasers at deep subwavelength scale. *Nature* **2009**, *461*, 629−632.

(8) De Leon, I.; Berini, P. Amplification of long-range surface plasmons by a dipolar gain medium. *Nat. Photonics* **2010**, *4*, 382−387.

(9) Gather, M. C.; Meerholz, K.; Danz, N.; Leosson, K. Net optical gain in a plasmonic waveguide embedded in a fluorescent polymer. *Nat. Photonics* **2010**, *4*, 457−461.

(10) Nezhad, M. P.; et al. Room-temperature subwavelength metallo-dielectric lasers. *Nat. Photonics* **2010**, *4*, 395−399.

(11) Ma, R. M.; Oulton, R. F.; Sorger, V. J.; Bartal, G.; Zhang, X. Room-temperature sub-diffraction-limited plasmon laser by total internal reflection. *Nat. Mater.* **2011**, *10*, 110−113.

(12) Lu, Y. J.; et al. Plasmonic nanolaser using epitaxially grown silver film. *Science* **2012**, *337*, 450−453.

(13) Liu, N.; et al. Plasmonic amplification with ultra-high optical gain at room temperature. *Sci. Rep.* **2013**, *3*, 1967.

(14) Suh, J. Y.; et al. Plasmonic Bowtie Nanolaser Arrays. *Nano Lett.* **2012**, *12*, 5769−5774.

(15) Cubukcu, E.; Kort, E. A.; Crozier, K. B.; Capasso, F. Plasmonic laser antenna. *Appl. Phys. Lett.* **2006**, *89*, 093120.

(16) Maier, S. A. *Plasmonics: fundamentals and applications*; Springer: New York, 2007.

(17) MacDonald, K. F.; Sámson, Z. L.; Stockman, M. I.; Zheludev, N. I. Ultrafast active plasmonics. *Nat. Photonics* **2008**, *3*, 55−58.

(18) Chang, D. E.; Sørensen, A. S.; Hemmer, P. R.; Lukin, M. D. Quantum optics with surface plasmons. *Phys. Rev. Lett.* **2006**, *97*, 053002.

(19) Akimov, A. V.; et al. Generation of single optical plasmons in metallic nanowires coupled to quantum dots. *Nature* **2007**, *450*, 402−406.

(20) Chang, D. E.; Sørensen, A. S.; Hemmer, P. R.; Lukin, M. D. Strong coupling of single emitters to surface plasmons. *Phys. Rev. B* **2007**, *76*, 035420.

(21) Falk, A. L.; et al. Near-field electrical detection of optical plasmons and single-plasmon sources. *Nat. Phys.* **2009**, *5*, 475−479.

(22) Kolesov, R.; et al. Wave−particle duality of single surface plasmon polaritons. *Nat. Phys.* **2009**, *5*, 470−474.

(23) Schlather, A. E.; Large, N.; Urban, A. S.; Nordlander, P.; Halas, N. J. Near-Field Mediated Plexcitonic Coupling and Giant Rabi Splitting in Individual Metallic Dimers. *Nano Lett.* **2013**, *13*, 3281−3286.

(24) Murray, B. J.; Walter, E. C.; Penner, R. M. Amine Vapor Sensing with Silver Mesowires. *Nano Lett.* **2004**, *4*, 665−670.

(25) Anker, J. N.; Hall, W. P.; Lyandres, O.; Shah, N. C.; Zhao, J.; Van Duyne, R. P. Biosensing with plasmonic nanosensors. *Nat. Mater.* **2008**, *7*, 442−453.

(26) Fang, Y. R.; Wei, H.; Hao, F.; Nordlander, P.; Xu, H. X. Remote-excitation surface-enhanced Raman scattering using propagating Ag nanowire plasmons. *Nano Lett.* **2009**, *9*, 2049−2053.

(27) Piliarik, M.; Homola, J. Surface plasmon resonance (SPR) sensors: approaching their limits? *Opt. Express* **2009**, *17*, 16505−16517.

(28) Pacifici, D.; Lezec, H. J.; Atwater, H. A. All-optical modulation by plasmonic excitation of CdSe quantum dots. *Nat. Photonics* **2007**, *1*, 402−406.

(29) Pala, R. A.; Shimizu, K. T.; Melosh, N. A.; Brongersma, M. L. A Nonvolatile Plasmonic Switch Employing Photochromic Molecules. *Nano Lett.* **2008**, *8*, 1506−1510.

(30) Yan, R. X.; Gargas, D.; Yang, P. D. Nanowire photonics. *Nat. Photonics* **2009**, *3*, 569−576.

(31) Ditlbacher, H.; et al. Silver nanowires as surface plasmon resonators. *Phys. Rev. Lett.* **2005**, *95*, 257403.

(32) Kusar, P.; Gruber, C.; Hohenau, A.; Krenn, J. R. Measurement and Reduction of Damping in Plasmonic Nanowires. *Nano Lett.* **2012**, *12*, 661−665.

(33) West, P. R.; Ishii, S.; Naik, G. V.; Emani, N. K.; Shalaev, V. M.; Boltasseva, A. Searching for better plasmonic materials. *Laser Photon. Rev.* **2010**, *4*, 795−808.
(34) Piccione, B.; van Vugt, L. K.; Agarwal, R. Propagation Loss Spectroscopy on Single Nanowire Active Waveguides. *Nano Lett.* **2010**, *10*, 2251−2256.
(35) Xiao, Y.; et al. Single-Nanowire Single-Mode Laser. *Nano Lett.* **2011**, *11*, 1122−1126.
(36) Xiao, Y.; Meng, C.; Wu, X. Q.; Tong, L. M. Single mode lasing in coupled nanowires. *Appl. Phys. Lett.* **2011**, *99*, 023109.
(37) Guo, X.; et al. Direct Coupling of Plasmonic and Photonic Nanowires for Hybrid Nanophotonic Components and Circuits. *Nano Lett.* **2009**, *9*, 4515−4519.
(38) Shegai, T.; et al. Unidirectional Broadband Light Emission from Supported Plasmonic Nanowires. *Nano Lett.* **2011**, *11*, 706−711.
(39) Maslov, A.; Ning, C. Reflection of guided modes in a semiconductor nanowire laser. *Appl. Phys. Lett.* **2003**, *83*, 1237−1239.
(40) Wang, Z. Y.; Lu, Q. F.; Fang, X. S.; Tian, X. K.; Zhang, L. D. Manipulation of the morphology of CdSe nanostructures: the effect of Si. *Adv. Funct. Mater.* **2006**, *16*, 661−666.
(41) Tong, L. M.; et al. Assembly of Silica Nanowires on Silica Aerogels for Microphotonic Devices. *Nano Lett.* **2005**, *5*, 259−262.
(42) Sun, Y. G.; Xia, Y. N. Large-scale synthesis of uniform silver nanowires through a soft, self-seeding, polyol process. *Adv. Mater.* **2002**, *14*, 833−837.
(43) Zimmler, M. A.; Bao, J.; Capasso, F.; Muller, S.; Ronning, C. Laser action in nanowires: Observation of the transition from amplified spontaneous emission to laser oscillation. *Appl. Phys. Lett.* **2008**, *93*, 051101.
(44) Zhang, S. P.; et al. Chiral surface plasmon polaritons on metallic nanowires. *Phys. Rev. Lett.* **2011**, *107*, 096801.
(45) Wang, Y. P.; Ma, Y. G.; Guo, X.; Tong, L. M. Single-mode plasmonic waveguiding properties of metal nanowires with dielectric substrates. *Opt. Express* **2012**, *20*, 19006−19015.
(46) Rewitz, C.; et al. Ultrafast Plasmon Propagation in Nanowires Characterized by Far-Field Spectral Interferometry. *Nano Lett.* **2011**, *12*, 45−49.